

Dips in the Diffuse Supernova Neutrino Background

Yasaman Farzan^{a 1} and Sergio Palomares-Ruiz^{b 2}

^a *School of physics, Institute for Research in Fundamental Sciences (IPM),
P.O.Box 19395-5531, Tehran, Iran*

^b *Instituto de Física Corpuscular (IFIC), CSIC-Universitat de València,
Apartado de Correos 22085, E-46071 Valencia, Spain*

Abstract

Scalar (fermion) dark matter with mass in the MeV range coupled to ordinary neutrinos and another fermion (scalar) is motivated by scenarios that establish a link between radiatively generated neutrino masses and the dark matter relic density. With such a coupling, cosmic supernova neutrinos, on their way to us, could resonantly interact with the background dark matter particles, giving rise to a dip in their redshift-integrated spectra. Current and future neutrino detectors, such as Super-Kamiokande, LENA and Hyper-Kamiokande, could be able to detect this distortion.

¹ yasaman@theory.ipm.ac.ir

² Sergio.Palomares.Ruiz@ific.uv.es

I. INTRODUCTION

Core-collapse supernova (SN) explosions of type II, Ib and Ic are known sources of neutrinos with energies in the range of few to tens of MeV. If a SN explosion occurs in our galaxy at a distance of 10 kpc, over 10^4 events can be observed in current detectors such as Super-Kamiokande (SK) [1] or the proposed detectors such as LENA [2] as well as in the liquid scintillator detector to be installed in the ANDES observatory [3]. In addition, the IceCube neutrino telescope would register about 10^6 photons in excess of its background. Moreover, a number of smaller existing and upcoming detectors can collect tens to hundreds of SN events [4, 5]. However, galactic core-collapse SN events are rare [1, 6] and many years might pass before registering such an explosion in our galaxy.

On the other hand, the diffuse SN neutrino background (DSNB), from all the SN explosions that have occurred in the history of the Universe, is a guaranteed flux. The DSNB flux depends on the cosmic star formation rate [7–9], which is relatively well known up to redshift $z \simeq 9$ [7, 10]. Although so far there is only an upper bound on this diffuse neutrino flux [11–14], the limits are very close to the expectations from recent theoretical predictions [8, 15–32]. The proposed Gadolinium-doped SK phase [33], currently under study within the EGADS project [34], and the LENA detector [2] could detect up to $\sim 10 \bar{\nu}_e$ events per year. The proposed Hyper-Kamiokande (HK) detector, with a fiducial volume 25 times larger than SK [35], will be able to detect ~ 200 events per year. If the IceCube extension MICA is ever built [36], with a volume of ~ 5 Mton and a low energy threshold, $\mathcal{O}(1000)$ events per year could be collected. Thus, it is in principle possible to foresee that we will be able to reconstruct the $\bar{\nu}_e$ energy spectrum of the DSNB, which not only would allow us to constrain the SN models, but also to search for unexpected surprises.

As it is well known [37–42], the spectrum of neutrinos with extremely high energies (i.e., $E_\nu = m_Z^2/(2m_\nu) > 10^{21}$ eV) could be distorted by the resonant interaction off cosmic relic neutrinos at the Z -pole. In a similar fashion, neutrinos from cosmological core-collapse SN events may interact on their way to Earth with the intergalactic matter leading to a deformation of their spectrum. For instance, in models with additional light Z' gauge bosons coupled to neutrinos, SN neutrinos could interact with the low energy relic neutrino background giving rise to a dip in their spectrum [43, 44]. In this paper, we show that if the dark matter (DM) consists of a scalar (fermion) of mass in the MeV range or lower, with Yukawa couplings to neutrinos and another new fermion (scalar) with a mass of a few MeV, the *en-route* resonant interaction of the DSNB neutrinos with DM could also lead to a dip in the spectrum. Such mass range and couplings are motivated by models in which neutrino masses are generated radiatively [45–47]. Although different theoretical models

predict slightly different shapes for the DSNB spectra, they are all smooth spectra. Thus, a sharp feature, such as a dip, would be a clear signature of new physics [48–51]. Here we mainly discuss the effects on the DSNB spectra, although we also mention the signature from a galactic SN.

The paper is organized as follows. In Sec. II, we present the scenario and review various bounds on its parameters. In Sec. III, we discuss the resonance absorption of the DSNB and formulate the conditions for having a significant dip in the spectrum. In Sec. IV, we discuss the evolution of the flux, present the numerical results on the effect of the new coupling on the DSNB spectrum and show the expected spectrum of events at a detector such as HK. In Sec. V, we review our results and its implications for new physics and conclude.

II. NEUTRINO INTERACTIONS WITH DARK MATTER

Let us suppose that neutrinos have a coupling of form

$$gN_R^\dagger\nu_L\phi, \quad (1)$$

with a new scalar ϕ and a new fermion N_R , which are both neutral and have a mass in the MeV range. Of course, this coupling can be only effective below the electroweak scale. Various minimal models to embed the coupling within a theory invariant under $SU(3) \times SU(2) \times U(1)$ have been proposed [46, 52, 53]. In addition, if the whole Lagrangian is invariant under a Z_2 symmetry ($N \rightarrow -N$, $\phi \rightarrow -\phi$ and SM \rightarrow SM), the lightest of the particles ϕ and N would be a DM candidate. The right-handed neutrino N can be either of Dirac type or of Majorana type. The limiting case of pseudo-Dirac N , as discussed below, is of particular interest. The scalar particle ϕ can be either real or complex. In each case, two situations are possible: $m_\phi < m_N$ or $m_N < m_\phi$. Thus, there are in general eight possibilities.

The SLIM scenario [45–47], which links the neutrino mass with the DM relic density, corresponds to the case that $m_\phi < m_N$ with ϕ being real and N Majorana. In this scenario, the light neutrino masses are obtained at loop level and the annihilation channels $\phi\phi \rightarrow \nu\nu, \bar{\nu}\bar{\nu}$ determine the DM abundance. Taking the observed value of the DM abundance and neutrino masses in the range $\sqrt{\Delta m_{\text{atm}}^2} \sim 0.05 \text{ eV} - 1 \text{ eV}$, it was found that the mass of N is in the $\sim 1\text{--}10$ MeV range [45–47]. The mass of ϕ would therefore be in the MeV range or lower.

There are a number of different observables that set bounds on the coupling constants. The coupling in Eq. (1) can lead to new decay modes for charged leptons and charged mesons such as K^+ and π^+ . In particular, it can lead to $K^+ \rightarrow e^+ + N + \phi$ and also $K^+ \rightarrow \mu^+ + N + \phi$, which would appear as decay into charged leptons plus missing energy.

As long as $\max\{m_\phi^2, m_N^2\} \ll m_{K,\pi}^2$, this discussion is similar for all the eight possibilities enumerated above. The present bounds are $|g_e|^2 < 10^{-5}$ [54] and $|g_\mu|^2 < 10^{-4}$ [55, 56]. These bounds could be improved by KLOE [57] and NA62 [58] data. Of course, these bounds do not apply if the sum of the masses of ϕ and N is larger than the kaon mass. For $m_K < m_\phi + m_N < m_D$, the strongest bound on g_e comes from the D meson decay modes: $|g_e| < 0.4$ [59, 60]. From the W boson decay modes [60] we find $g_\mu, g_e < 1$. The bound on the coupling of ν_τ is much weaker as the τ leptons are not produced in the kaon decays. The strongest bound in this case comes from τ decays [59]. In fact g_τ can be as large as $\mathcal{O}(1)$.

If ϕ is real and N is of Majorana type, the active neutrino mass would receive a contribution at one loop level. The upper bound on masses of the active neutrinos then yields $g < 10^{-3}$ [45–47]. If ϕ is complex or N is of Dirac type, the lepton number would be conserved so there would be no contribution to active neutrino masses. A more interesting scenario is the case with pseudo-Dirac N and real ϕ . Let us restore flavor indices and assume a $U(1) \times U(1) \times U(1)$ flavor symmetry softly broken only by $(m_R)_{\alpha\beta}$. The flavor symmetry dictates that for any flavor ν_α there is a separate Dirac N_α with mass $m_{N_\alpha} \bar{N}_\alpha N_\alpha$ and coupling g_α . The flavor structure of the light active neutrinos would be given by

$$(m_\nu)_{\alpha\beta} \simeq \frac{g_\alpha g_\beta}{4\pi} (m_R)_{\alpha\beta} \log\left(\frac{\Lambda^2}{m_{\phi,N}^2}\right), \quad (2)$$

where Λ is the cutoff scale above which the effective coupling in Eq. (1) is not valid (i.e., electroweak scale) and $m_{\phi,N}^2$ is a linear combination of $m_{N_\alpha}^2$, $m_{N_\beta}^2$ and m_ϕ^2 of order of $(1-10)^2$ MeV². By taking m_R small enough, the bounds on the coupling from the mass of active neutrinos can be relaxed. Notice that even with $g_\mu \ll g_\tau$, we can obtain $(m_\nu)_{\mu\mu} \sim (m_\nu)_{\tau\tau}$ provided that $(m_R)_{\mu\mu} \gg (m_R)_{\tau\tau}$. Similar considerations hold for $g_e \ll g_\tau$. Unless stated otherwise, in the following, by N we mean N_τ , which has the strongest coupling.

The coupling in Eq. (1) also leads to the annihilation of a DM pair. If we require the DM production in the early universe to be thermal, the total annihilation cross section should be $\mathcal{O}(1)$ pb. As discussed in detail in the Appendix, for all the cases discussed above this requirement implies $g \ll 0.1$, except when N is of (pseudo-)Dirac type and the DM candidate is a real scalar with $m_\phi < m_N$. Such a small coupling ($g \ll \mathcal{O}(0.1)$) would not give a detectable dip in the DSNB (see below). As a result, we focus on the case with real ϕ and pseudo-Dirac N in our analysis, for which couplings $\mathcal{O}(0.1)$ are consistent with the thermal DM scenario. All in all, the overall behavior of our results for the rest of the aforementioned cases is similar.

In addition, the cosmic microwave background data as well as the data on big bang nucleosynthesis can set a lower bound on DM mass of the order of MeV. However, in the case of a real ϕ as a DM candidate these bounds are relaxed [61]. Stable particles in the

MeV range coupled to neutrino could also contribute to SN cooling. Within the present uncertainties in the SN models, a real MeV mass scalar might be tolerated.

In summary, we will focus on the case with N being of pseudo-Dirac type and real ϕ playing the role of DM coupled dominantly to ν_τ . This setup escapes all the present bounds. For simplicity, with the purpose of clearly illustrating the effects under discussion, in this work we only consider a single ϕ and a single N . In principle, in addition to active light neutrinos there can be sterile neutrinos (ν_s) coupled to N and ϕ : $g_s N_R^\dagger \nu_s \phi$. The g_s coupling can be as large as $\mathcal{O}(1)$, increasing the decay width of N dramatically. We will briefly discuss the implications of this case, too.

III. RESONANT ABSORPTION OF SUPERNOVA RELIC NEUTRINOS

Following the discussion of the previous section, we will consider a general coupling of neutrinos and DM given by $g_i \nu_i \phi N$, where ν_i represent mass eigenvalues of active neutrinos. There are two subtleties here: (1) As we saw in the previous section, for ϕ and N with masses in the MeV range, only the ν_τ coupling can be significant, which means $g_i \propto U_{\tau i}$; (2) as discussed in the previous section, reproducing the neutrino mass structure requires more than one N . Recalling that the couplings of N_e and N_μ are severely constrained by meson decay experiments, their effects on the DSNB spectrum cannot be large. We therefore drop them from our discussion and focus on effects of a single N .

If the center-of-mass energy of the neutrino-DM system corresponds to the N -pole (ϕ -pole), a resonant absorption along the propagation of the DSNB would occur, giving rise to a dip in the predicted flux. In this section, we formulate the conditions under which the absorption dip can be significant. Following the discussion in the previous section, we assume that DM is composed of ϕ . Similar consideration holds for $m_N < m_\phi$ with N as the DM candidate. Thus, we use m_r and m_{DM} to refer to the mass of the particle produced at resonance (in our case m_N) and the DM mass (in our case m_ϕ), respectively.

The resonance neutrino energy in the laboratory frame, E_r , is

$$E_r = \frac{m_r^2 - m_{\text{DM}}^2}{2 m_{\text{DM}}} = E_0 (1 + z_r) , \quad (3)$$

where E_0 is the energy of the relic neutrino observed at Earth and z_r is the redshift at which the resonant interaction occurred. In the above expression, we have neglected the very small momenta of the DM particles due to nonzero temperature ($T/m_{\text{DM}} \ll 1$) and considered them to be at rest.

The optical depth τ for the cosmic propagation of a relic SN neutrino is given by

$$\tau = \int \frac{c dt}{\lambda_\nu} = \int dz \frac{dt}{dz} n(z) \sigma(z), \quad (4)$$

where $\lambda_\nu = (n\sigma)^{-1}$ is the mean-free path of the relic SN neutrino, $n(z)$ is the DM density, $\sigma(z)$ is the neutrino-DM interaction cross section and $dt/dz = -((1+z)H(z))^{-1}$ is the time-redshift relation. For the epoch of interest,

$$H(z) \simeq H_0 \sqrt{\Omega_\Lambda + \Omega_{\text{m},0}(1+z)^3}. \quad (5)$$

with the present value of the Hubble parameter $H_0 = (67.3 \pm 1.2) \times \text{km sec}^{-1}\text{Mpc}^{-1}$ and $\Omega_\Lambda = 0.685_{-0.016}^{+0.018}$ and $\Omega_{\text{m},0} = 0.315_{-0.018}^{+0.016}$ [62].

The probability for a SN relic neutrino not to undergo interaction during its cosmic propagation is given by $e^{-\tau}$, so the absorbed fraction of flux, f_{abs} , is given by $f_{\text{abs}} = 1 - e^{-\tau}$. Hence, in order to determine the parameter range over which significant dips in the DSNB flux could be produced, we should impose some condition on f_{abs} (or equivalently on τ).

The average DM density at any z is given in terms of the present density by

$$n(z) = n_0 (1+z)^3 = \frac{\Omega_{\text{DM},0} \rho_c}{m_{\text{DM}}} (1+z)^3 \simeq 1.26 \left(\frac{\text{keV}}{m_{\text{DM}}} \right) (1+z)^3 \text{ cm}^{-3} \quad (6)$$

where $\rho_c = 3H_0^2/(8\pi G_N) = 4.77 \text{ keV}/\text{cm}^3$ is the critical density of the Universe and $\Omega_{\text{DM},0} = 0.265$ is the present fraction of DM [62].

Since the non-resonant processes have negligible effects for the DSNB absorption¹, we shall only consider the s-channel contribution to the cross section. For the case when the intermediate resonance particle decays isotropically in its rest frame (e.g., if it is a scalar), the decay of the resonance produces a flat final neutrino spectrum over the interval $E_{\text{min}} \leq E'_\nu \leq E_\nu$. We can therefore write the differential cross section as

$$\frac{d\sigma_{ij}^p}{dE'_\nu}(E_\nu, E'_\nu) = \sigma_{ij}^p(E_\nu) \frac{\theta(E_\nu - E'_\nu)}{E_\nu - E_{\text{min}}} \theta(E'_\nu - E_{\text{min}}), \quad (7)$$

where the superindex $p = \text{LC, LV}$ refers to the lepton number conserving (LC) or lepton number violating (LV) scattering, $E_{\text{min}} = m_{\text{DM}} E_\nu / (2E_\nu + m_{\text{DM}})$ and θ is the step function. The i (j) subindex refers to the incoming (outgoing) neutrino. However, in our case N (being a fermion) decays non-isotropically. In general, one can write

$$\frac{d\sigma_{ij}^p}{dE'} = \frac{d\sigma_{ij}^p}{d \cos \theta} \frac{2E_\nu + m_{\text{DM}}}{E_\nu^2} \quad (8)$$

¹ The non-resonant part can be estimated as $\sigma_{\text{nr}} \sim g^4/(16\pi E_\nu^2)$ so $\tau_{\text{nr}} \sim \int dz (dt/dz) n(z) \sigma_{\text{nr}}(z) \sim 4g^4$, which is negligible for $g < 0.5$.

where $d\sigma_{ij}^p/d\cos\theta$ is the partial scattering cross section in the center of mass frame of ϕ - N system and

$$\frac{m_{\text{DM}}}{2E_\nu + m_{\text{DM}}}E_\nu < E'_\nu < E_\nu . \quad (9)$$

Close to the resonance energy, the cross section of $\nu_i\phi \rightarrow N \rightarrow \nu_j\phi$ is given by

$$\frac{d\sigma_{ij}^{\text{LC}}}{d\cos\theta} = \frac{g_i^2 g_j^2}{32\pi} \frac{(m_r^2 - m_{\text{DM}}^2)^2}{(m_r^2 + m_{\text{DM}}^2)} \frac{1 + \cos\theta}{(s - m_r^2)^2 + \Gamma_r^2 m_r^2} , \quad (10)$$

where Γ_r is the decay width of the particle produced at resonance (in our case N) and s is the Mandelstam variable, $s = 2m_{\text{DM}}E_\nu + m_{\text{DM}}^2$ in which E_ν is the energy of ν at the interaction.

If N is of Majorana type, in addition to LC scattering $\nu_i\phi \rightarrow N \rightarrow \nu_j\phi$, we can have $\nu_i\phi \rightarrow N \rightarrow \bar{\nu}_j\phi$ as well as $\bar{\nu}_i\phi \rightarrow N \rightarrow \nu_j\phi$ with

$$\frac{d\sigma_{ij}^{\text{LV}}}{d\cos\theta} = \frac{g_i^2 g_j^2}{32\pi} \frac{(m_r^2 - m_{\text{DM}}^2)^2}{(m_r^2 + m_{\text{DM}}^2)} \frac{1 - \cos\theta}{(s - m_r^2)^2 + \Gamma_r^2 m_r^2} . \quad (11)$$

Of course, for Dirac N and complex ϕ , lepton number is conserved and the channel corresponding to Eq. (11) is forbidden. As discussed in the Appendix, in the pseudo-Dirac case, practically for each pair (N_R, N_L) , there are two quasi-degenerate mass eigenstates N_1 and N_2 with couplings $g/\sqrt{2}$ and $ig/\sqrt{2}$, so their contributions to the LV process approximately cancel each other. Thus, the LV processes for the pseudo-Dirac scenario can be neglected. Having two mass eigenvectors, there should be, in principle, two resonances. However if the mass difference is much smaller than Γ_r , the two peaks cannot be resolved and the LC cross section is given mainly by Eq. (10). If the active neutrino masses are produced by couplings as those in Eq. (1), from Eq. (2) we conclude $|m_{N_1} - m_{N_2}|/\Gamma_r = 0.06(m_\nu/0.05 \text{ eV})(\text{MeV}/m_N)(0.1/g_i)^4 \ll 1$, so we are in the limit that we can safely use Eq. (10).

Close to the resonance, the total LC cross section is given by

$$\sigma_{ij}(s) \simeq \frac{g_i^2 g_j^2}{16\pi} \frac{(m_r^2 - m_{\text{DM}}^2)^2}{m_r^2 + m_{\text{DM}}^2} \frac{1}{(s - m_r^2)^2 + \Gamma_r^2 m_r^2} . \quad (12)$$

Notice that for Majorana N , the cross section is twice as much the one in Eq. (12). If the main decay mode of N is to $\phi\nu$, we obtain

$$\Gamma_r = \sum_i \frac{g_i^2}{16\pi} \frac{(m_r^2 - m_{\text{DM}}^2)^2}{m_r^3} . \quad (13)$$

For $\Gamma_r \ll m_r$, it is convenient to use the narrow width approximation limit to analytically

solve Eq. (4). Thus, the cross section can be written as

$$\begin{aligned}\sigma_{ij}(s) &\simeq \frac{g_i^2 g_j^2}{\sum_k g_k^2} \pi \frac{m_r^2}{m_r^2 + m_{\text{DM}}^2} \delta(s - m_r^2) \\ &= \frac{g_i^2 g_j^2}{\sum_k g_k^2} \pi \frac{1+z}{m_r^2 - m_{\text{DM}}^2} \frac{m_r^2}{m_r^2 + m_{\text{DM}}^2} \delta\left((1+z) - \frac{m_r^2 - m_{\text{DM}}^2}{2m_{\text{DM}} E_0}\right).\end{aligned}\quad (14)$$

Inserting Eqs. (5), (6) and (14) into Eq. (4), the optical depth for a given neutrino mass eigenstate emitted at a redshift of z_r with an energy of $E_0(1+z_r)$ can be analytically calculated. For $E_0 \leq E_r$, we have

$$\begin{aligned}\tau_i(z_r) &= \sum_j \frac{g_i^2 g_j^2}{\sum_k g_k^2} \left(\frac{\pi}{m_r^2 - m_{\text{DM}}^2}\right) \left(\frac{m_r^2}{m_r^2 + m_{\text{DM}}^2}\right) \left(\frac{n_0}{H_0}\right) \left(\frac{\Omega_{\text{DM}}(z_r)}{\Omega_{\text{DM},0}}\right) \\ &\simeq 5 \times 10^2 g_i^2 \left(\frac{20 \text{ MeV}}{E_r}\right) \left(\frac{\text{MeV}}{m_{\text{DM}}}\right)^2 \left(\frac{E_r + m_{\text{DM}}/2}{E_r + m_{\text{DM}}}\right) \left(\frac{\Omega_{\text{DM}}(z_r)}{\Omega_{\text{DM},0}}\right),\end{aligned}\quad (15)$$

where $\Omega_{\text{DM}}(z) = \Omega_{\text{DM},0}(1+z)^3/\sqrt{\Omega_\Lambda + \Omega_{\text{m},0}(1+z)^3}$. Notice that the fraction of DM, $\Omega_{\text{DM}}(z)$, is a monotonously increasing function with $\Omega_{\text{DM}}(0) = \Omega_{\text{DM},0}$ and $\Omega_{\text{DM}}(6) = 32.9 \Omega_{\text{DM},0}$.

For a minimal absorption of $f_{\text{abs}} = 10\%$, we obtain the condition

$$g_i^2 > 2 \times 10^{-4} \left(\frac{E_r}{20 \text{ MeV}}\right) \left(\frac{m_{\text{DM}}}{\text{MeV}}\right)^2 \left(\frac{\Omega_{\text{DM},0}}{\Omega_{\text{DM}}(z_r)}\right) \left(\frac{E_r + m_{\text{DM}}}{E_r + m_{\text{DM}}/2}\right).\quad (16)$$

In Fig. 1, assuming $E_r \gg m_{\text{DM}}$, we show the absorbed fraction of the flux at the resonance energy as a function of the coupling for two redshifts. As seen from the figure, while for $g_i \lesssim 10^{-2} (E_r/20 \text{ MeV})^{1/2} (m_{\text{DM}}/\text{MeV})$, the absorption at $z = 0$ is negligible, for slightly larger values of the coupling, $g_i \gtrsim \text{few} \times 10^{-2} (E_r/20 \text{ MeV})^{1/2} (m_{\text{DM}}/\text{MeV})$, the absorption becomes significant. Increasing the redshift, absorption for a given coupling becomes stronger, but occurs at a lower observed energy. The sharp dependence on the coupling reflects the exponential dependence of f_{abs} on g_i^2 .

So far we have considered the cumulative absorption of the DSNB. Nevertheless, the DM density in halos is much larger than the average DM density in the Universe, so one could wonder whether neutrinos produced by a SN in our own galaxy, traveling towards us in a medium with high DM density, will experience similar effects. In fact, the optical depth for neutrinos in the Milky Way could be much larger than the one corresponding to cosmological distances with average density given by Eq. (6). However, only neutrinos with energies in a very narrow interval, $(E_r - \Gamma_r m_r/2m_{\text{DM}}, E_r + \Gamma_r m_r/2m_{\text{DM}})$, would undergo resonant scattering. Thus, as long as $\Gamma_r m_r/2m_{\text{DM}} \ll O(1) \text{ MeV}$, one can neglect the effect of resonant neutrino absorption in the DM halo of the Milky Way because the dip would be smeared due to the finite energy resolution of the detector. Let us note however that, if

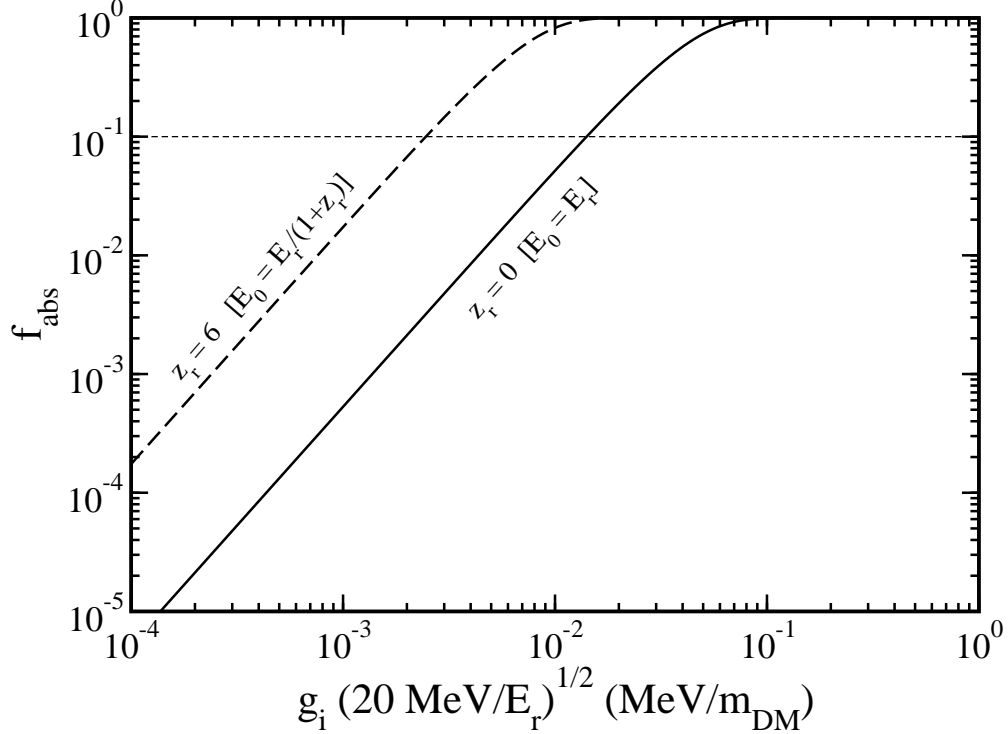


Figure 1: The absorbed fraction of the flux at the resonance energy, $f_{\text{abs}}(z_r) = 1 - e^{-\tau_i(z_r)}$, as a function of the coupling for two different redshifts. The thin dashed line indicates 10% absorption. Here we assume $E_r \gg m_{\text{DM}}$.

the resonantly produced particle (N in this case) has other decay modes which increase Γ_r to $O(1)\text{MeV}$, this effect might be detectable. One example can be N decaying to ϕ and a sterile neutrinos ν_s with $\Gamma(N \rightarrow \nu_s \phi) \sim 1 \text{ MeV}$.

In a similar way, SN explosions at cosmological distances have also taken place inside galaxies, so right after their production, neutrinos traverse a medium with a much higher DM density than the average cosmic background. Thus, large resonant absorption at the host galaxy at redshift z is expected to occur in the observed energy interval $(E_r/(1+z) - \Gamma_r/(1+z)m_r/2m_{\text{DM}}, E_r/(1+z) + \Gamma_r/(1+z)m_r/2m_{\text{DM}})$. However, for a very narrow resonance, the fraction of the flux which is absorbed at the host is so small that it amounts to a very small suppression of the cumulated flux. This is unlike the case of the redshift-integrated effect in the DSNB for which all energies between E_r and $E_r/(1+z)$ experience resonant absorption at some point on their way from the host at z to us.

IV. NEUTRINO SPECTRA AND EVENTS

Let us consider the process in which a neutrino of mass m_i , with energy $\mathcal{E}_z = E_\nu(1+z)$ hits a DM particle ϕ and resonantly produces N at redshift z . Subsequently, in the case of lepton number conserving (violating) processes, N decays into a neutrino (antineutrino) of mass m_j , with energy $\mathcal{E}'_z = E'_\nu(1+z)$ and a DM particle ϕ , i.e., $\nu_i\phi \rightarrow N \rightarrow \nu_j\phi$ ($\nu_i\phi \rightarrow N \rightarrow \bar{\nu}_j\phi$). Taking Φ_i ($\Phi_{\bar{i}}$) as the neutrino (antineutrino) flux of mass m_i , let us define

$$F_i(t, E_\nu) \equiv \frac{d\Phi_i}{dE_\nu}(t, E_\nu) . \quad (17)$$

The time evolution of $F_i(t, E_\nu)$ is then governed by (see, e.g., Ref. [63])

$$\begin{aligned} \frac{\partial F_i(t, E_\nu)}{\partial t} = & -3H(t)F_i(t, E_\nu) + \frac{\partial}{\partial E_\nu} (H(t)E_\nu F_i(t, E_\nu)) - \frac{1}{\lambda_i(t, E_\nu)} F_i(t, E_\nu) \\ & + \sum_j \int_{E_\nu}^{\infty} dE'_\nu \left[\mathcal{T}_{ji}^{\text{LC}}(t, E'_\nu, E_\nu) F_j(t, E'_\nu) + \mathcal{T}_{ji}^{\text{LV}}(t, E'_\nu, E_\nu) F_{\bar{j}}(t, E'_\nu) \right] \\ & + \mathcal{L}_i(t, E_\nu)/a^3(t) , \end{aligned} \quad (18)$$

where $\mathcal{L}_i(t, E_\nu)$ in the last term is the comoving luminosity of the source of neutrinos of mass m_i and

$$\lambda_i(t, E_\nu) \equiv \frac{1}{\sum_{p,j} n(t) \sigma_{ij}^p(E_\nu)} \quad ; p = \text{LC, LV} \quad (19)$$

$$\mathcal{T}_{ji}^{\text{LC}}(t, E'_\nu, E_\nu) \equiv n(t) \frac{d\sigma_{ji}^{\text{LC}}}{dE_\nu}(E'_\nu, E_\nu) \quad (20)$$

$$\mathcal{T}_{ji}^{\text{LV}}(t, E'_\nu, E_\nu) \equiv n(t) \frac{d\sigma_{\bar{j}i}^{\text{LV}}}{dE_\nu}(E'_\nu, E_\nu) . \quad (21)$$

In the right hand side of Eq. (18), the first and second terms originate from the expansion of the Universe and the induced adiabatic energy losses, respectively. The third term represents the absorption dip, where $\lambda_i(t, E_\nu)$ is the mean-free path of neutrinos of mass m_i given in Eq. (19). In Eq. (19), $n(t)$ is the number density of the DM particles at time t , Eq. (6), and σ_{ij}^p is the total cross section of the considered process ($p=\text{LC, LV}$). The fourth term in Eq. (18) represents the repopulation of the spectrum at energies lower than the resonance energy, where the contributions from both LC and LV processes are included. Obviously, for observed energies at the Earth larger than the resonance energy, the original spectrum does not suffer distortion, but just becomes redshifted. Finally, the fifth term in Eq. (18) represents the luminosity of the sources.

The comoving luminosity of the source of neutrinos of flavor α at redshift z , $\mathcal{L}_\alpha(z, E_\nu)$, is given by

$$\mathcal{L}_\alpha(z, E_\nu) = R_{\text{SN}}(z) F_\alpha^{\text{SN}}(E_\nu) \quad (22)$$

	\overline{E}_{ν_e} [MeV]	$\overline{E}_{\bar{\nu}_e}$ [MeV]	\overline{E}_{ν_x} [MeV]	β_{ν_e}	$\beta_{\bar{\nu}_e}$	β_{ν_x}
Model A [19]	11.2	15.4	21.6	2.8	3.8	1.8
Model B [31, 32]	10	12	15	3	3	2.4

Table I: Parameters for the different neutrino spectra according to the parameterization given in Eq. (24), for two different models. The luminosity of the different flavors for both models are taken to be $L_{\nu_e} = L_{\bar{\nu}_e} = L_{\nu_x} = 5.0 \times 10^{52}$ ergs.

where $F_\alpha^{\text{SN}}(E_\nu)$ is the number spectrum of neutrinos of flavor α emitted by a typical SN and $R_{\text{SN}}(z)$ represents the SN rate per comoving volume at redshift z .

For the SN rate per comoving volume we invoke canonical parameters for optically luminous core-collapse SN ($M_{\text{min}} = 8M_\odot$ and $M_{\text{max}} = 40M_\odot$) [9] and use the fit to the star formation rate from the combination of low- z ultraviolet and far infrared data [7] and from high- z galaxies and gamma-ray bursts data, assuming a Salpeter initial mass function, obtained by Ref. [10],

$$R_{\text{SN}}(z) = 0.0088 M_\odot^{-1} \dot{\rho}_0 \left[(1+z)^{a\zeta} + \left(\frac{1+z}{B}\right)^{b\zeta} + \left(\frac{1+z}{C}\right)^{c\zeta} \right]^{1/\zeta}, \quad (23)$$

with $\dot{\rho}_0 = 0.02 M_\odot \text{ yr}^{-1} \text{ Mpc}^{-3}$, $a = 3.4$, $b = -0.3$, $c = -2.5$, $\zeta = -10$, $B = (1+z_1)^{1-a/b}$ and $C = (1+z_1)^{(b-a)/c} (1+z_2)^{1-b/c}$ in which $z_1 = 1$ and $z_2 = 4$.

For the neutrino spectrum from a typical SN, we consider the parameterization for each flavor given by [65]

$$F_\alpha^{\text{SN}}(E_\nu) = \frac{(1+\beta_{\nu_\alpha})^{1+\beta_{\nu_\alpha}} L_{\nu_\alpha}}{\Gamma(1+\beta_{\nu_\alpha}) \overline{E}_{\nu_\alpha}^2} \left(\frac{E_\nu}{\overline{E}_{\nu_\alpha}}\right)^{\beta_{\nu_\alpha}} e^{-(1+\beta_{\nu_\alpha})E_\nu/\overline{E}_{\nu_\alpha}}. \quad (24)$$

Below, we show results for two sets of parameters. We take the optimistic case from the simulation of the Lawrence Livermore group [19] (model A) with relatively high average energies: $\overline{E}_{\nu_e} = 11.2$ MeV, $\overline{E}_{\bar{\nu}_e} = 15.4$ MeV, $\overline{E}_{\nu_x} = 21.6$ MeV; $\beta_{\nu_e} = 2.8$, $\beta_{\bar{\nu}_e} = 3.8$, $\beta_{\nu_x} = 1.8$; $L_{\nu_e} = L_{\bar{\nu}_e} = L_{\nu_x} = 5.0 \times 10^{52}$ ergs [24], in which ν_x represents non-electron-flavor neutrinos and antineutrinos. Notice however that this simulation overlooks some relevant neutrino processes. Recent simulations indicate lower average energies for the $\bar{\nu}_e$ and ν_x flavors. Hence, we also study model B with $\overline{E}_{\nu_e} = 10$ MeV, $\overline{E}_{\bar{\nu}_e} = 12$ MeV, $\overline{E}_{\nu_x} = 15$ MeV; $\beta_{\nu_e} = 3$, $\beta_{\bar{\nu}_e} = 3$, $\beta_{\nu_x} = 2.4$; $L_{\nu_e} = L_{\bar{\nu}_e} = L_{\nu_x} = 5.0 \times 10^{52}$ ergs [31, 32]. The parameters are summarized in Tab. I.

Neutrino fluxes arise from the central regions of the collapsed star where the density is very high and the effective neutrino mixings are therefore strongly suppressed. For the measured

values of the neutrino mixing parameters, the propagation inside the star is adiabatic. Thus, at the surface of the star, the fluxes of mass eigenstates can be identified with the flavor fluxes at production². In the case of normal hierarchy (NH) for the neutrino mass ordering, $\bar{\nu}_e$ (ν_e) is coincident with $\bar{\nu}_1$ (ν_3), whereas in the case of inverted hierarchy (IH), $\bar{\nu}_e$ (ν_e) coincides with $\bar{\nu}_3$ (ν_2), so in terms of the neutrinos with definite mass, the SN spectra are [64]

$$\begin{aligned} F_{\bar{\nu}_1}^{\text{SN}}(E_\nu) &= F_{\bar{\nu}_e}^{\text{SN}}; & F_{\bar{\nu}_2}^{\text{SN}}(E_\nu) &= F_{\nu_x}^{\text{SN}}; & F_{\bar{\nu}_3}^{\text{SN}}(E_\nu) &= F_{\nu_x}^{\text{SN}} \\ F_{\nu_1}^{\text{SN}}(E_\nu) &= F_{\nu_x}^{\text{SN}}; & F_{\nu_2}^{\text{SN}}(E_\nu) &= F_{\nu_x}^{\text{SN}}; & F_{\nu_3}^{\text{SN}}(E_\nu) &= F_{\nu_e}^{\text{SN}}, \end{aligned} \quad (25)$$

for NH, and

$$\begin{aligned} F_{\bar{\nu}_1}^{\text{SN}}(E_\nu) &= F_{\nu_x}^{\text{SN}}; & F_{\bar{\nu}_2}^{\text{SN}}(E_\nu) &= F_{\nu_x}^{\text{SN}}; & F_{\bar{\nu}_3}^{\text{SN}}(E_\nu) &= F_{\bar{\nu}_e}^{\text{SN}} \\ F_{\nu_1}^{\text{SN}}(E_\nu) &= F_{\nu_x}^{\text{SN}}; & F_{\nu_2}^{\text{SN}}(E_\nu) &= F_{\nu_e}^{\text{SN}}; & F_{\nu_3}^{\text{SN}}(E_\nu) &= F_{\nu_x}^{\text{SN}}, \end{aligned} \quad (26)$$

for IH.

The solution to Eq. (18) for neutrinos (and equivalently for antineutrinos) in terms of neutrino mass eigenstates is given by (see, e.g., Ref. [66]):

$$\begin{aligned} F_i(z, E_\nu) &= (1+z)^2 \int_z^{z_{\text{max}}} \frac{dz'}{H(z')} e^{-\int_z^{z'} \frac{dz''}{(1+z'')H(z'')} \frac{1}{\lambda_i(z'', \mathcal{E}_{z''})}} \times \left\{ \mathcal{L}_i(z', \mathcal{E}_{z'}) \right. \\ &\quad \left. + \sum_j \int_{\mathcal{E}_{z'}}^{\infty} d\mathcal{E}'_{z'} \left[\mathcal{T}_{ji}^{\text{LC}}(z', \mathcal{E}'_{z'}, \mathcal{E}_{z'}) F_j(z', \mathcal{E}'_{z'}) + \mathcal{T}_{ji}^{\text{LV}}(z', \mathcal{E}'_{z'}, \mathcal{E}_{z'}) F_{\bar{j}}(z', \mathcal{E}'_{z'}) \right] \right\} \end{aligned} \quad (27)$$

where we take $z_{\text{max}} = 6$. Note that most of the signal comes from SN explosions at $z < 1$, so the exact upper limit for the redshift is not crucial.

Finally, the spectrum of neutrinos of flavor α at Earth is given by

$$F_\alpha(z=0, E_\nu) = \sum_i |U_{\alpha i}|^2 F_i(z=0, E_\nu). \quad (28)$$

where U is the PMNS neutrino mixing matrix. We use $\sin^2 \theta_{12} = 0.306$, $\sin^2 \theta_{23} = 0.446$ (0.587), $\sin^2 \theta_{13} = 0.0229$ and $\delta = 0$ for NH (IH) [67] (see also Refs. [68, 69]).

In Fig. 2 we show the resulting integrated $\bar{\nu}_e$ spectra for model A (left panels) and model B (right panels) for the two neutrino mass hierarchies³. We show the spectra after cosmological absorption and redistribution to lower energies (thick solid lines), with no absorption considered (thin solid lines) and with absorption, but without flux redistribution

² Let us note that neutrino-neutrino collective effects introduce corrections below the 10% level on the DSNB, with no energy-dependent signatures due to smearing over time and over the SN population [31].

In this work, we neglect this small correction.

³ For the numerical calculations we use Eqs. (10)-(12).

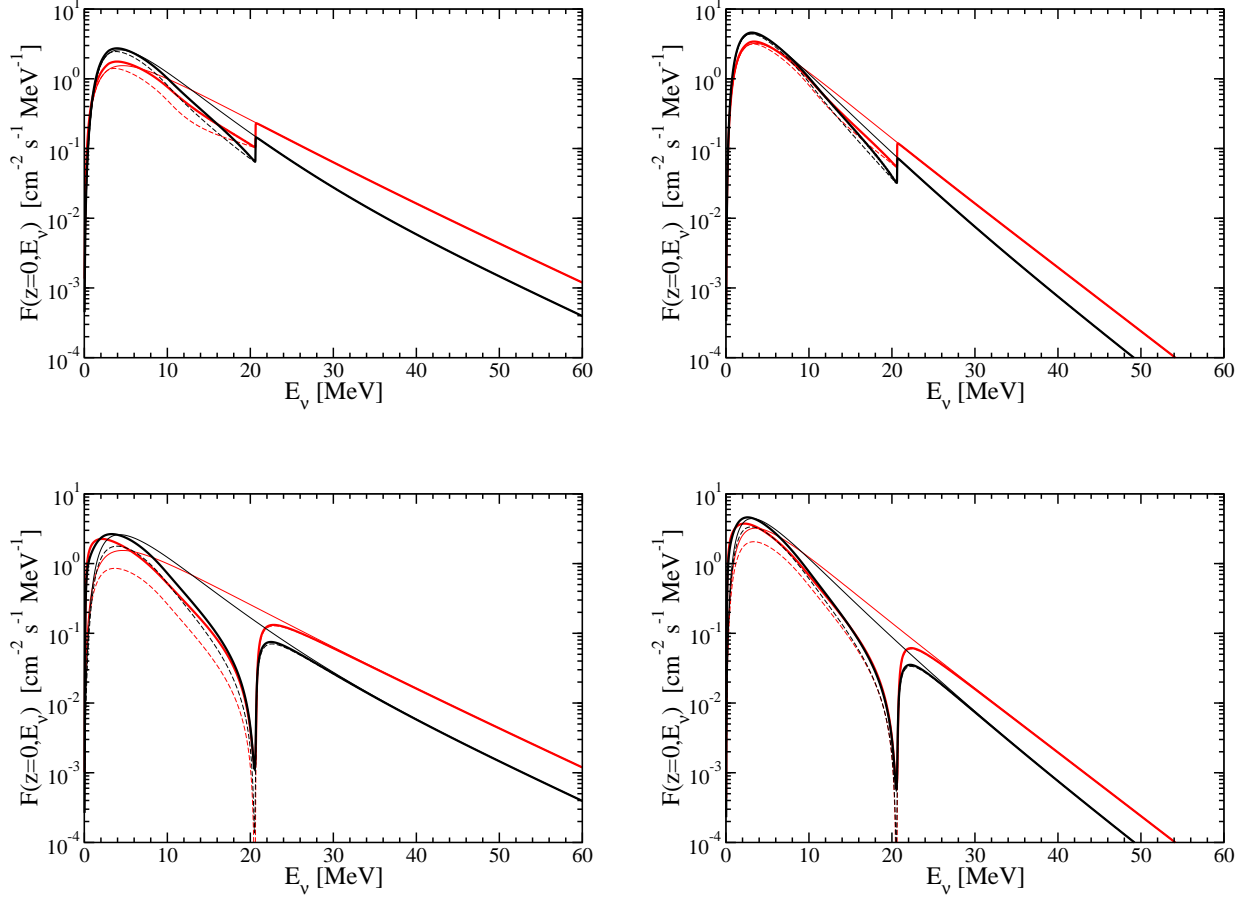


Figure 2: DSNB $\bar{\nu}_e$ spectra for model A (left panels) and model B (right panels), assuming $g_\tau = 0.1$ (upper panels) and $g_\tau = 0.5$ (lower panels). In the four panels, we assume $m_\phi = m_{\text{DM}} = 1$ MeV, $m_N = m_\tau = 6.5$ MeV (Dirac) and $g_e = g_\mu = 0$, for NH (lower black lines at high energies) and IH (upper red lines at high energies). The effect of the redshift-integrated absorption is depicted by the thick solid lines. The case of no absorption is represented by thin solid lines, whereas dashed lines do not include the redistribution of the flux to lower energies after the interaction (e.g., $\bar{\nu}_i\phi \rightarrow N \rightarrow \bar{\nu}_s\phi$).

(dashed lines). The absence of flux redistribution takes place e.g., when the decay of N is dominated by a coupling to sterile neutrinos: $\bar{\nu}_i\phi \rightarrow N \rightarrow \bar{\nu}_s\phi$. We consider N to be a Dirac particle and assume $m_\phi = m_{\text{DM}} = 1$ MeV, $m_N = m_\tau = 6.5$ MeV ($E_\tau = 20.6$ MeV) and $g_e = g_\mu = 0$, $g_\tau = 0.1$ (upper panels) and $g_\tau = 0.5$ (lower panels). In the mass basis, the couplings read $g_1 = g_\tau U_{\tau 1} \simeq 0.03$, $g_2 = g_\tau U_{\tau 2} \simeq 0.06$ and $g_3 = g_\tau U_{\tau 3} \simeq 0.07$. Notice that although g_e is taken to be zero, the spectrum of $\bar{\nu}_e$ is affected due to neutrino mixing. The figures show that, as expected, the distortion of the spectrum starts at the resonance energy. The dip is broadened due to the absorption at different redshifts. Above ~ 10 MeV the flux

is higher for the case of IH. This can be easily understood from Eqs. (25), (26) and (28). In the case of IH, the observed $\bar{\nu}_e$ flux is dominated by the ν_x component ($|U_{e3}|^2 \simeq 0.02$), which has the highest average temperature, whereas in the case of NH, $\sim 70\%$ ($|U_{e1}|^2 \simeq 0.7$) of the original $\bar{\nu}_e$ flux survives. Thus, the final $\bar{\nu}_e$ flux at Earth in the case of IH is higher above approximately the average energy of the original $\bar{\nu}_e$ spectrum⁴. Likewise, model A provides a higher flux than model B at high energies due to its higher average energies.

Let us now consider the expected signal in a future water-Čerenkov detector like HK [35]. In Fig. 3 we depict the expected number of events per year in 2-MeV bins for the cases shown in Fig. 2. We assume a fiducial volume of 562.5 kton (25 times the volume used in the DSNB searches in SK), a constant detection efficiency of 90% and an energy resolution of 10% over the whole visible (positron/electron) energy range, which are typical SK parameters [13, 14, 73–75]. Although the main signal comes from inverse beta decay events ($\bar{\nu}_e + p \rightarrow e^+ + n$), we also add the contribution from the interactions of ν_e and $\bar{\nu}_e$ off Oxygen nuclei, as done in Refs. [70–72]. In Fig. 3, the dotted vertical line indicates the current SK energy threshold, which is mainly set by the large number of spallation products. However, adding Gd would make the neutron tagging of the inverse beta decay neutrons efficient [33], which could be used to significantly reduce backgrounds and move the detection threshold to lower energies. Thus, we extend the event spectra down to 10 MeV.

We see that for $g_\tau = 0.5$ (lower panels), in all the cases, even for the SK threshold of 16 MeV, the drop in the event spectrum below the resonance energy is very significant. On the other hand, for $g_\tau = 0.1$, in the case of IH and model A, the dip is also very likely to be detectable (even once backgrounds are properly added and a full analysis performed). This would signal the presence of new physics producing a suppression with respect to the expected DSNB flux. For the other cases and $g_\tau = 0.1$, the suppression of the expected flux is also significant. However it might be non trivial to disentangle this signal from a spectrum with lower average energies. For this less favorable case ($g_\tau = 0.1$) and the assumed parameters, we expect a $\sim 25\%$ ($\sim 15\%$) effect in the whole energy range considered in Fig. 3 for a threshold energy of 10 MeV (16 MeV), whereas for $g_\tau = 0.5$, we expect a suppression of $\sim 50\%$ ($\sim 40\%$). On the other hand, the suppression when only considering the bins affected by the resonant interaction is $\sim 35\%$ ($\sim 30\%$) for $g_\tau = 0.1$, and $\sim 65\%$ ($\sim 60\%$) for $g_\tau = 0.5$. In the less optimistic scenario, i.e., $g_\tau = 0.1$, model B and NH, HK would detect ~ 11 (~ 35) events/year in the energy interval $16 \text{ MeV} < E_{\text{vis}} < 22 \text{ MeV}$ ($10 \text{ MeV} < E_{\text{vis}} < 22 \text{ MeV}$) as compared to the ~ 16 (~ 50) events/year when no absorption occurs. In the most optimistic scenario, i.e., $g_\tau = 0.5$, model A and IH, HK would detect ~ 16

⁴ Note that the total luminosity is the same in all flavors.

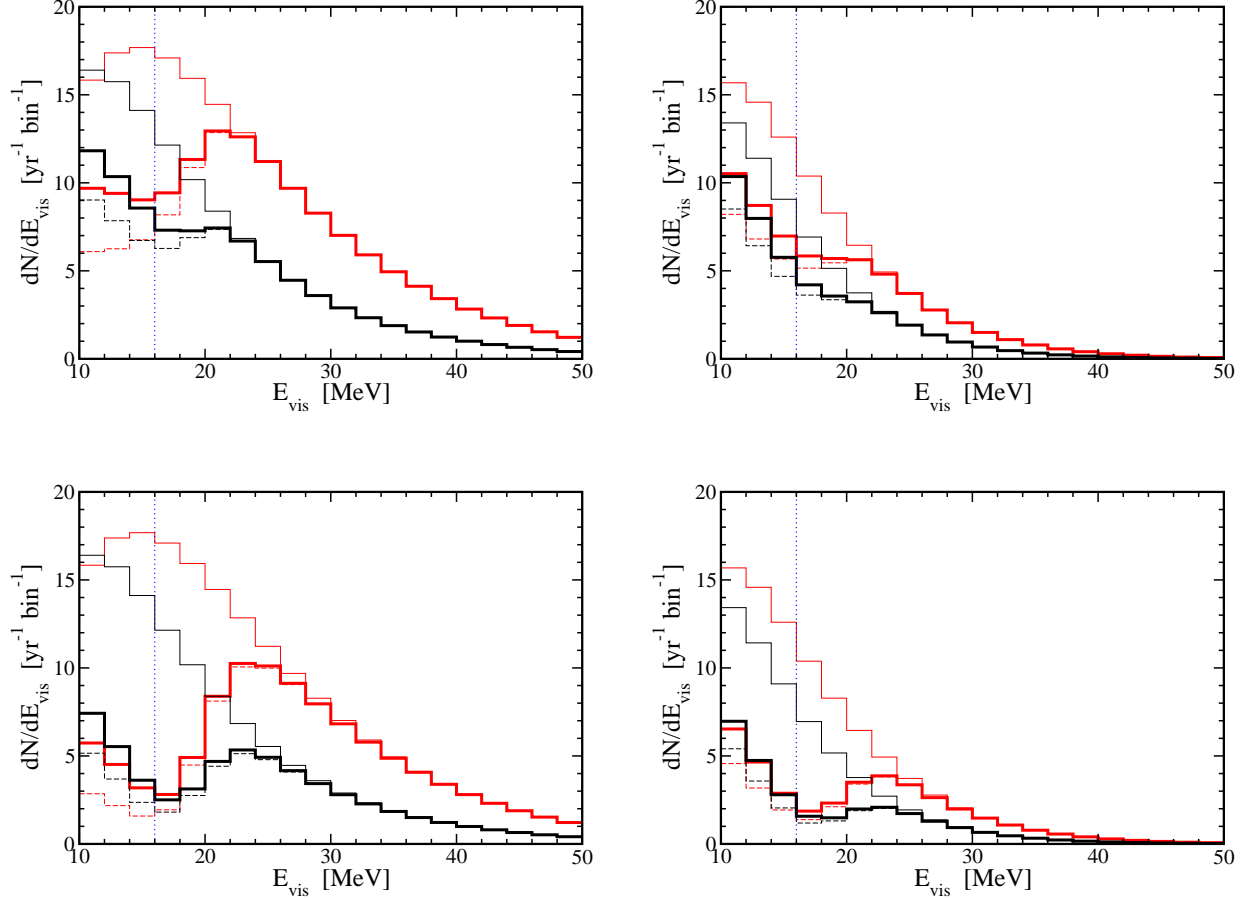


Figure 3: *Event spectra at HK for model A (left panels) and model B (right panels), assuming $g_\tau = 0.1$ (upper panels) and $g_\tau = 0.5$ (lower panels). The common parameters and explanation of the curves are the same as those in Fig. 2. We assume a fiducial volume of 562.5 kton ($25 \times SK$), a constant detection efficiency of 90% and an energy resolution of 10% over the whole visible (positron/electron) energy range. The vertical dotted line is the current SK threshold. E_{vis} represents the energy of the detected positron/electron.*

(~ 30) events/year as compared to the ~ 47 (~ 98) events/year when there is no absorption. Hence, if a resonance of this type occurs in the relevant energy range, after a few years, it could be possible to determine the presence of the redshift-integrated resonance dip with a reasonable confidence level. Let us note that a detailed statistical analysis including all the relevant backgrounds for different experimental setups (with or without Gd) is beyond the scope of this work.

Let us finally mention that in a liquid scintillator detector like the proposed LENA [2], tagging inverse beta decay events is possible by the delayed coincidence between the prompt positron and the gamma-ray from neutron capture. Therefore, the only irreducible back-

grounds are reactor and atmospheric $\bar{\nu}_e$, and hence, LENA would have a low energy threshold (~ 10 MeV) and twice the number of protons of SK (about ten times fewer than HK). In addition, LENA would also be sensitive to all flavors via neutral-current reactions as neutrino-proton or neutrino-electron elastic scattering, although the statistics for these channels is at least an order of magnitude lower, making the corresponding rate of the DSNB very low for the study of the spectral features discussed in this work.

In the examples considered so far, we have taken $g_e = g_\mu = 0$ because for light ϕ and N , there are strong bounds on these couplings from kaon decay data, below which the distortion of the DSNB spectrum is negligible. However, as discussed before for $m_\phi + m_N > m_K$, the bounds from kaon decays on g_e and g_μ can be relaxed. For such masses, to have a resonance energy below ~ 30 MeV, a fine tuned cancelation between m_ϕ^2 and m_N^2 is needed (see Eq. (3)). In addition, the optical depth at resonance goes as $g^2/(E_r m_{\text{DM}}^2)$ and hence the magnitude of the dip is very much suppressed. We have studied the distortion of the spectrum for $m_\phi = m_{\text{DM}} = 240$ MeV, $m_N = m_\tau = 260$ MeV (for which $E_r = 20.8$ MeV) and $g_e = g_\mu = 0.4$ and found that the effect of the interaction is negligible.

V. CONCLUSIONS

We have studied the distortion of the energy spectrum of DSNB within scenarios with DM, with mass in the MeV range, coupled to ordinary neutrinos ν as $gN_R^\dagger\nu_L\phi$ with the lighter new particle (a scalar ϕ or a heavy neutrino N) playing the role of DM. We have found that such a coupling could give rise to a resonance scattering of neutrinos off the ambient DM background. Although the resonance would be in general very narrow, the cumulative effect of resonance scattering of neutrinos at different redshifts could lead to a significantly wide dip in the spectrum at the detectors. In order to have a sizeable effect, the coupling should be relatively large $g > \text{few} \times 10^{-2}(E_r/20 \text{ MeV})^{1/2}(m_{\text{DM}}/\text{MeV})$. The overall results are the same for all eight cases with $m_N < m_\phi$ or $m_\phi > m_N$; ϕ being real or complex and N being (pseudo-)Dirac or Majorana. We have however focused on the case with real ϕ and (pseudo-)Dirac N , for this is the only case for which the annihilation cross section of the DM pair remains below the thermal limit (i.e., ~ 1 pb) even for couplings as large as $g \sim \mathcal{O}(1)$. Nevertheless, relaxing the the constraints on the couplings imposed by the thermal scenario, other lepton number conserving cases with large couplings could also be possible.

Strong upper bounds on the g_e and g_μ couplings are also imposed from studies of meson decays. The bounds apply for all the eight cases mentioned above, provided the sum of the masses of N and ϕ to be below the kaon mass. In order to avoid these bounds, we have

focused on the following case: coupling exclusively to ν_τ , i.e., $g_e = g_\mu = 0$ and $g_\tau \neq 0$). We have also considered the case $g_e \neq 0$; $g_\mu \neq 0$, when $m_N + m_\phi > m_K$ with $E_R < 30$ MeV (see Eq. (3)), although the expected dip is very small. For the lepton number violating case (Majorana N and real ϕ), the coupling induces a contribution to neutrino mass at one-loop level so the upper bound on active neutrino masses can be translated into a strong upper bound on the coupling. We have shown that in the limiting case of pseudo-Dirac N and real ϕ , the active neutrino mass matrix could be reconstructed at one-loop level despite the relatively large coupling giving rise to the distortion of the energy spectrum of the DSNB.

When $E_\tau \sim 20$ MeV and $g > 0.1$, the distortion of the spectrum is quite sizeable. The ability of a detector to establish the presence of the dip depends on the statistics, and hence, on the detector mass and energy threshold. We have studied two models for the SN neutrino spectra (see Tab. I). As is well known, the statistics also depends on the neutrino mass hierarchy. For IH, the number of $\bar{\nu}_e$ events would be higher. We have found that for the favorable case of model A and IH, the presence of the dip could be established after a few years of data taking by the upcoming HK detector, clearly indicating the role of new physics at play. For the less favorable case of NH, the deviation of the spectrum from the prediction of a specific SN model could be established, but the distortion could be hidden within the uncertainties on the SN model, i.e., because of the statistical errors, the effect of the dip in the spectrum of the observed events could be reproduced by shifting the average neutrino energies to lower values. Nevertheless, a detailed statistical analysis including all the backgrounds and parametrizations of the SN neutrino spectra is beyond the scope of this work. We have also discussed the prospects of the proposed LENA experiment, although its smaller size would render spectral analyses challenging.

If the presence of the dip is established, such a feature would indicate the presence of new physics. The question would be then whether one could establish the particular scenario and coupling we have assumed. The shape of the dip could be indicative of a resonance scattering *en route* and could not be reproduced by other new physics scenarios such as pseudo-Dirac neutrino oscillation [76, 77]. However, other scenarios giving rise to resonance scattering (like scattering on the background relic neutrinos via an s-channel light Z' exchange [43, 44]) could give rise to a similar feature. Even with low energy experiments such as those studying the meson or lepton decays, distinguishing between the two scenarios would be challenging because they predict a similar deviation from the SM expectations. In order to distinguish between these two cases, one should look for the signatures of the ultraviolet complete model embedding these scenarios.

Acknowledgments

We thank T. Weiler for a careful reading of the manuscript. SPR is supported by a Ramón y Cajal contract and by the Spanish MINECO under grant FPA2011-23596. YF and SPR are also partially supported by the European Union FP7 ITN INVISIBLES (Marie Curie Actions, PITN-GA-2011-289442). SPR was also partially supported by the Portuguese FCT through the projects CERN/FP/123580/2011, PTDC/FIS-NUC/0548/2012 and CFTP-FCT Unit 777 (PEst-OE/FIS/UI0777/2013), which are partially funded through POCTI (FEDER). SPR gratefully acknowledges the hospitality and financial support of the Institute for Research in Fundamental Sciences (IPM), where parts of this work were done.

Appendix: DM annihilation cross section

In this section, we study the annihilation of dark matter pair via the coupling in Eq. (1). The mass term for N_R can in general be written as

$$(N_R^T \ N_L^T)c \begin{pmatrix} m_R & m_D \\ m_D & m_L \end{pmatrix} \begin{pmatrix} N_R \\ N_L \end{pmatrix}. \quad (29)$$

We denote the mass eigenvalues by m_N . In the case $m_R, m_L = 0$ ($\ll m_D$), N_R is a (pseudo-)Dirac fermion. Otherwise, N_R is a Majorana fermion and the presence of N_L is unnecessary. Lepton number is conserved if ϕ is complex and/or N is of Dirac type.

In the pseudo-Dirac limit, mass eigenstates are almost degenerate Majorana fermions. We denote the two mass eigenstates by

$$N_1 \simeq \frac{(1 + \alpha)N_L + (1 - \alpha)N_R}{\sqrt{2}} \quad \text{and} \quad N_2 \simeq i \frac{(1 - \alpha)N_L - (1 + \alpha)N_R}{\sqrt{2}}, \quad (30)$$

with $\alpha = (m_L - m_R)/2m_D$. The corresponding mass eigenvalues are

$$m_{N_1} = m_D + \frac{m_L + m_R}{2} \quad \text{and} \quad m_{N_2} = m_D - \frac{m_L + m_R}{2}. \quad (31)$$

Notice that substituting N_R with $((1 - \alpha)N_1 + i(1 + \alpha)N_2)/\sqrt{2}$ in Eq. (1), we find that the couplings of N_1 and N_2 are respectively equal to $g/\sqrt{2}$ and $ig/\sqrt{2}$.

Let us now discuss the annihilation of DM pairs for the eight possible cases mentioned in the text.

- *Case $m_N < m_\phi$* : In this case N is the DM candidate. Let us discuss the four possible subcases one by one:

– *Real ϕ and Dirac N* : In this LC case we have

$$\sigma(N N \rightarrow \nu \nu) = \sigma(\bar{N} \bar{N} \rightarrow \bar{\nu} \bar{\nu}) = \frac{g^4}{4\pi} \frac{m_N^2}{(m_N^2 + m_\phi^2)^2}. \quad (32)$$

Moreover, the $N\bar{N} \rightarrow \nu\bar{\nu}$ annihilation mode is an s-wave and is also given by

$$\langle \sigma(N\bar{N} \rightarrow \nu\bar{\nu})v \rangle = \frac{g^4 m_N^2}{4\pi(m_N^2 + m_\phi^2)^2}. \quad (33)$$

– *Real ϕ and Majorana N* : In this case, lepton number is violated and a pair of N 's can annihilate into $\nu\nu$ with the annihilation cross section given by Eq. (32). On the other hand, LC annihilation into $\nu\bar{\nu}$ is p-wave suppressed and therefore subdominant (see Eq. (34)).

– *Complex ϕ and Dirac N* : The LV annihilation into $\nu\nu$ or $\bar{\nu}\bar{\nu}$ pairs is forbidden, but LC pair annihilation into $\nu\bar{\nu}$ is allowed with a s-wave cross section given by Eq. (33).

– *Complex ϕ and Majorana N* : The dominant annihilation mode is the p-wave suppressed LC annihilation into a $\nu\bar{\nu}$ pair:

$$\langle \sigma(NN \rightarrow \nu\bar{\nu})v \rangle = \frac{4g^4}{3\pi} \frac{m_N^4 + m_\phi^4}{(m_N^2 + m_\phi^2)^4} p_{\text{DM}}^2, \quad (34)$$

where p_{DM} is the momentum of the DM at freeze-out: $p_{\text{DM}}^2 \sim m_N^2/20$.

Let us now comment on the pseudo-Dirac scenario with the mass eigenstates N_1 and N_2 and small mass splitting $\Delta m_N = m_L + m_R$. In early universe, these particles scatter off ϕ and ν with a rate given by $\Gamma_{\text{scat}} \sim g^4 T/4\pi$. At scattering, the final state is the chiral N_R , which is a coherent combination of N_1 and N_2 . As long as Δm_N is small enough to have $\Delta m_N/\Gamma_{\text{scat}} \ll 1$, coherence between mass eigenstates N_1 and N_2 is preserved, so DM pairs would interact with each other as Dirac particles. In the opposite case of $\Delta m_N/\Gamma_{\text{scat}} \gg 1$, the coherence is lost and the N_1 and N_2 pairs annihilate and coannihilate with each other as Majorana particles.

If we want to restrict to the thermal DM scenario, the total annihilation cross section should be $\mathcal{O}(1)$ pb. Thus, in all cases with N as thermal DM, the values of the couplings should be $g < \mathcal{O}(0.01)$.

- *Case $m_\phi < m_N$* : In this case, which is extensively studied in Refs. [45–47], ϕ is the DM candidate. Let us consider the four different possibilities mentioned in Sec. II. If N is of Majorana type, regardless of whether ϕ is real or complex, the LV annihilation

channel $\phi\phi \rightarrow \nu\nu$ can take place. For real ϕ , we have $\sigma(\phi\phi \rightarrow \nu\nu) = \sigma(\phi\phi \rightarrow \bar{\nu}\bar{\nu})$ while for complex ϕ , we have $\sigma(\phi\phi \rightarrow \nu\nu) = \sigma(\bar{\phi}\bar{\phi} \rightarrow \bar{\nu}\bar{\nu})$. If we restrict the possibility to the thermal DM scenario, the total annihilation cross section should be $\mathcal{O}(1)$ pb, so the sum of these annihilation cross sections cannot exceed this value. Taking $m_L = 0$, $m_D \ll m_R$ (see Eq. (29)) and $m_N \simeq m_R \sim 1 - 10$ MeV, from $\sigma(\phi\phi \rightarrow \overset{(-)}{\nu}\overset{(-)}{\nu}) \sim 1$ pb, it was found in Refs. [45–47] that

$$3 \times 10^{-4} < g < 10^{-3} . \quad (35)$$

These LV modes are forbidden for Dirac N . For the pseudo-Dirac scenario, $\sigma(\phi\phi \rightarrow \nu\nu)$ is suppressed by $(m_R/m_D)^2$. As a result, by taking m_R/m_D arbitrarily small, the upper bound in Eq. (35) can be avoided. However, for both Dirac and Majorana N , if ϕ is complex, there would be p-wave annihilation into a $\nu\bar{\nu}$ pair: $\sigma(\phi\bar{\phi} \rightarrow \nu\bar{\nu}) \sim g^4 p_{DM}^2 / [4\pi(m_\phi^2 + m_N^2)^2]$. Taking $p_{DM}^2 \sim m_\phi^2/20$ at freeze-out, from $\langle\sigma(\phi\bar{\phi} \rightarrow \nu\bar{\nu})v\rangle \sim 1$ pb, we find $g \lesssim 0.01$. As discussed in Refs. [45–47], for real ϕ the cross section of annihilation into a $\nu\bar{\nu}$ pair is extremely suppressed, so this annihilation channel does not constrain significantly the coupling. Thus, for (pseudo-)Dirac N and real ϕ , there should be another coupling or mechanism to fix the DM abundance to the observed value.

In summary, if ϕ plays the role of DM, the bounds from imposing thermal production of DM (i.e., $\langle\sigma_{tot}v\rangle \sim \mathcal{O}(1)$ pb) constrain the coupling to be smaller than $\sim \mathcal{O}(0.01)$, unless ϕ is real and N is a (pseudo-)Dirac fermion. Of course, if the assumption of thermal production is relaxed, this bound does not apply anymore.

-
- [1] M. Ikeda *et al.* [Super-Kamiokande Collaboration], *Astrophys. J.* **669**, 519 (2007) [arXiv:0706.2283 [astro-ph]].
 - [2] M. Wurm *et al.* [LENA Collaboration], *Astropart. Phys.* **35**, 685 (2012) [arXiv:1104.5620 [astro-ph.IM]].
 - [3] P. A. N. Machado, T. Muhlbeier, H. Nunokawa and R. Zukanovich Funchal, *Phys. Rev. D* **86**, 125001 (2012) [arXiv:1207.5454 [hep-ph]].
 - [4] K. Scholberg, *Nucl. Phys. Proc. Suppl.* **221**, 248 (2011) [astro-ph/0701081].
 - [5] K. Scholberg, *J. Phys. Conf. Ser.* **203**, 012079 (2010).
 - [6] E. N. Alekseev and L. N. Alekseeva, *J. Exp. Theor. Phys.* **95**, 5 (2002) [*Zh. Eksp. Teor. Fiz.* **95**, 10 (2002)] [astro-ph/0212499].

- [7] A. M. Hopkins and J. F. Beacom, *Astrophys. J.* **651**, 142 (2006) [astro-ph/0601463].
- [8] S. Horiuchi, J. F. Beacom and E. Dwek, *Phys. Rev. D* **79**, 083013 (2009) [arXiv:0812.3157 [astro-ph]].
- [9] S. Horiuchi, J. F. Beacom, C. S. Kochanek, J. L. Prieto, K. Z. Stanek and T. A. Thompson, *Astrophys. J.* **738**, 154 (2011) [arXiv:1102.1977 [astro-ph.CO]].
- [10] M. D. Kistler, H. Yuksel and A. M. Hopkins, arXiv:1305.1630 [astro-ph.CO].
- [11] M. Malek *et al.* [Super-Kamiokande Collaboration], *Phys. Rev. Lett.* **90**, 061101 (2003) [hep-ex/0209028].
- [12] C. Lunardini and O. L. G. Peres, *JCAP* **0808**, 033 (2008) [arXiv:0805.4225 [astro-ph]].
- [13] K. Bays *et al.* [Super-Kamiokande Collaboration], *Phys. Rev. D* **85**, 052007 (2012) [arXiv:1111.5031 [hep-ex]].
- [14] K. Bays, Ph.D. Thesis, U. California, Irvine, 2012.
- [15] T. Totani and K. Sato, *Astropart. Phys.* **3**, 367 (1995) [astro-ph/9504015].
- [16] T. Totani, K. Sato and Y. Yoshii, *Astrophys. J.* **460**, 303 (1996) [astro-ph/9509130].
- [17] R. A. Malaney, *Astropart. Phys.* **7**, 125 (1997) [astro-ph/9612012].
- [18] D. H. Hartmann and S. E. Woosley, *Astropart. Phys.* **7**, 137 (1997).
- [19] T. Totani, K. Sato, H. E. Dalhed and J. R. Wilson, *Astrophys. J.* **496**, 216 (1998) [astro-ph/9710203].
- [20] M. Kaplinghat, G. Steigman and T. P. Walker, *Phys. Rev. D* **62**, 043001 (2000) [astro-ph/9912391].
- [21] S. Ando, K. Sato and T. Totani, *Astropart. Phys.* **18**, 307 (2003) [astro-ph/0202450].
- [22] M. Fukugita and M. Kawasaki, *Mon. Not. Roy. Astron. Soc.* **340**, L7 (2003) [astro-ph/0204376].
- [23] L. E. Strigari, M. Kaplinghat, G. Steigman and T. P. Walker, *JCAP* **0403**, 007 (2004) [astro-ph/0312346].
- [24] S. Ando, *Astrophys. J.* **607**, 20 (2004) [astro-ph/0401531].
- [25] S. Ando and K. Sato, *New J. Phys.* **6**, 170 (2004) [astro-ph/0410061].
- [26] F. Iocco, G. Mangano, G. Miele, G. G. Raffelt and P. D. Serpico, *Astropart. Phys.* **23**, 303 (2005) [astro-ph/0411545].
- [27] L. E. Strigari, J. F. Beacom, T. P. Walker and P. Zhang, *JCAP* **0504**, 017 (2005) [astro-ph/0502150].
- [28] C. Lunardini, *Astropart. Phys.* **26**, 190 (2006) [astro-ph/0509233].

- [29] F. Daigne, K. A. Olive, P. Sandick and E. Vangioni, Phys. Rev. D **72**, 103007 (2005) [astro-ph/0509404].
- [30] C. Lunardini, Phys. Rev. Lett. **102**, 231101 (2009) [arXiv:0901.0568 [astro-ph.SR]].
- [31] C. Lunardini and I. Tamborra, JCAP **1207**, 012 (2012) [arXiv:1205.6292 [astro-ph.SR]].
- [32] I. Tamborra, B. Muller, L. Hudepohl, H. -T. Janka and G. Raffelt, Phys. Rev. D **86**, 125031 (2012) [arXiv:1211.3920 [astro-ph.SR]].
- [33] J. F. Beacom and M. R. Vagins, Phys. Rev. Lett. **93**, 171101 (2004) [hep-ph/0309300].
- [34] H. Watanabe *et al.* [Super-Kamiokande Collaboration], Astropart. Phys. **31**, 320 (2009) [arXiv:0811.0735 [hep-ex]].
- [35] K. Abe *et al.*, arXiv:1109.3262 [hep-ex].
- [36] D. Cowen, talk at the Intensity Frontier Workshop, Argonne National Laboratory, Lemont, IL (USA), April 2013.
- [37] T. J. Weiler, Phys. Rev. Lett. **49**, 234 (1982).
- [38] T. J. Weiler, Astrophys. J. **285**, 495 (1984).
- [39] E. Roulet, Phys. Rev. D **47**, 5247 (1993).
- [40] S. Yoshida, H. -y. Dai, C. C. H. Jui and P. Sommers, Astrophys. J. **479**, 547 (1997) [astro-ph/9608186].
- [41] B. Eberle, A. Ringwald, L. Song and T. J. Weiler, Phys. Rev. D **70**, 023007 (2004) [hep-ph/0401203].
- [42] G. Barenboim, O. Mena Requejo and C. Quigg, Phys. Rev. D **71**, 083002 (2005) [hep-ph/0412122].
- [43] H. Goldberg, G. Perez and I. Sarcevic, JHEP **0611**, 023 (2006) [hep-ph/0505221].
- [44] J. Baker, H. Goldberg, G. Perez and I. Sarcevic, Phys. Rev. D **76**, 063004 (2007) [hep-ph/0607281].
- [45] C. Boehm, Y. Farzan, T. Hambye, S. Palomares-Ruiz and S. Pascoli, Phys. Rev. D **77**, 043516 (2008) [hep-ph/0612228].
- [46] Y. Farzan, Phys. Rev. D **80**, 073009 (2009) [arXiv:0908.3729 [hep-ph]].
- [47] Y. Farzan, Int. J. Mod. Phys. A **26**, 2461 (2011) [arXiv:1106.2948 [hep-ph]].
- [48] S. Palomares-Ruiz and T. J. Weiler, unpublished.
- [49] T. J. Weiler, talk at TeV Particle Astrophysics II, University of Wisconsin, Madison, WI (USA), August 2006.

- [50] S. Palomares-Ruiz, talk at WIN '07, Saha Institute, Kolkata (India), January 2007.
- [51] S. Palomares-Ruiz, talk at NUSKY 2011, ICTP, Trieste (Italy), June 2011.
- [52] E. Ma, Phys. Rev. D **73**, 077301 (2006) [hep-ph/0601225].
- [53] Y. Farzan, S. Pascoli and M. A. Schmidt, JHEP **1010**, 111 (2010) [arXiv:1005.5323 [hep-ph]].
- [54] F. Ambrosino *et al.* [KLOE Collaboration], Eur. Phys. J. C **64**, 627 (2009) [Erratum-ibid. **65**, 703 (2010)] [arXiv:0907.3594 [hep-ex]].
- [55] C. Y. Pang, R. H. Hildebrand, G. D. Cable and R. Stiening, Phys. Rev. D **8**, 1989 (1973).
- [56] Y. Farzan, Mod. Phys. Lett. A **25**, 2111 (2010) [arXiv:1009.1234 [hep-ph]].
- [57] <http://www.lnf.infn.it/kloe2>
- [58] <http://na62.web.cern.ch/NA62/Home/Home.html>
- [59] A. P. Lessa and O. L. G. Peres, Phys. Rev. D **75**, 094001 (2007) [hep-ph/0701068].
- [60] J. Beringer *et al.* [Particle Data Group Collaboration], Phys. Rev. D **86**, 010001 (2012).
- [61] C. Boehm, M. J. Dolan and C. McCabe, JCAP **1308**, 041 (2013) [arXiv:1303.6270 [hep-ph]].
- [62] P. A. R. Ade *et al.* [Planck Collaboration], arXiv:1303.5076 [astro-ph.CO].
- [63] V. Berezhinsky and A. Z. Gazizov, Astrophys. J. **643**, 8 (2006) [arXiv:astro-ph/0512090].
- [64] A. S. Dighe and A. Y. Smirnov, Phys. Rev. D **62**, 033007 (2000) [hep-ph/9907423].
- [65] M. T. Keil, G. G. Raffelt and H. -T. Janka, Astrophys. J. **590**, 971 (2003) [astro-ph/0208035].
- [66] M. Ahlers, L. A. Anchordoqui and S. Sarkar, Phys. Rev. D **79**, 083009 (2009) [arXiv:0902.3993 [astro-ph.HE]].
- [67] M. C. Gonzalez-Garcia, M. Maltoni, J. Salvado and T. Schwetz, JHEP **1212**, 123 (2012) [arXiv:1209.3023 [hep-ph]].
- [68] D. V. Forero, M. Tortola and J. W. F. Valle, Phys. Rev. D **86**, 073012 (2012) [arXiv:1205.4018 [hep-ph]].
- [69] G. L. Fogli, E. Lisi, A. Marrone, D. Montanino, A. Palazzo and A. M. Rotunno, Phys. Rev. D **86**, 013012 (2012) [arXiv:1205.5254 [hep-ph]].
- [70] S. Palomares-Ruiz and S. Pascoli, Phys. Rev. D **77**, 025025 (2008) [arXiv:0710.5420 [astro-ph]].
- [71] S. Palomares-Ruiz, Phys. Lett. B **665**, 50 (2008) [arXiv:0712.1937 [astro-ph]].
- [72] N. Bernal, J. Martín-Albo and S. Palomares-Ruiz, JCAP **1308**, 011 (2013) [arXiv:1208.0834 [hep-ph]].
- [73] J. Hosaka *et al.* [Super-Kamiokande Collaboration], Phys. Rev. D **73**, 112001 (2006) [hep-ex/0508053].

- [74] J. P. Cravens *et al.* [Super-Kamiokande Collaboration], Phys. Rev. D **78**, 032002 (2008) [arXiv:0803.4312 [hep-ex]].
- [75] K. Abe *et al.* [Super-Kamiokande Collaboration], Phys. Rev. D **83**, 052010 (2011) [arXiv:1010.0118 [hep-ex]].
- [76] J. F. Beacom, N. F. Bell, D. Hooper, J. G. Learned, S. Pakvasa and T. J. Weiler, Phys. Rev. Lett. **92**, 011101 (2004) [hep-ph/0307151].
- [77] A. Esmaili and Y. Farzan, JCAP **1212**, 014 (2012) [arXiv:1208.6012 [hep-ph]].